University of Nebraska - Lincoln
DigitalCommons@University of Nebraska - Lincoln

Papers in Natural Resources | Natural Resources, School of

12-13-2018

Assessing Responses of *Betula papyrifera* to Climate Variability in a Remnant Population along the Niobrara River Valley in Nebraska U.S. through Dendroecological and Remote Sensing Techniques

Evan Bumann
University of Nebraska - Lincoln, ebumann@huskers.unl.edu

Tala Awada
University of Nebraska - Lincoln, tawada2@unl.edu

Brian Wardlow
University of Nebraska-Lincoln, bwardlow2@unl.edu

Michael Hayes
University of Nebraska Lincoln, mhayes2@unl.edu

Jane A. Okalebo
University of Nebraska-Lincoln, JANE.OKALEBO@GMAIL.COM

See last page for additional authors

Follow this and additional works at: http://digitalcommons.unl.edu/natrespapers

Part of the Natural Resources and Conservation Commons, Natural Resources Management and Policy Commons, and the Other Environmental Sciences Commons

Bumann, Evan; Awada, Tala; Wardlow, Brian; Hayes, Michael; Okalebo, Jane A.; Helzer, C.; Mazis, Anastasios; Hiller, J.; and Cherubini, Paolo, "Assessing Responses of *Betula papyrifera* to Climate Variability in a Remnant Population along the Niobrara River Valley in Nebraska U.S. through Dendroecological and Remote Sensing Techniques" (2018). *Papers in Natural Resources*. 803.
http://digitalcommons.unl.edu/natrespapers/803

This Article is brought to you for free and open access by the Natural Resources, School of at DigitalCommons@University of Nebraska - Lincoln. It has been accepted for inclusion in Papers in Natural Resources by an authorized administrator of DigitalCommons@University of Nebraska - Lincoln.

Authors
Evan Bumann, Tala Awada, Brian Wardlow, Michael Hayes, Jane A. Okalebo, C. Helzer, Anastasios Mazis, J. Hiller, and Paolo Cherubini

This article is available at DigitalCommons@University of Nebraska - Lincoln: http://digitalcommons.unl.edu/natrespapers/803

Assessing Responses of *Betula papyrifera* to Climate Variability in a Remnant Population along the Niobrara River Valley in Nebraska U.S. through Dendroecological and Remote Sensing Techniques

E. BUMANN[1], T. AWADA[1*], B. WARDLOW[1], M. HAYES[1], J. OKALEBO[1], C. HELZER[2], A. MAZIS[1], J. HILLER[1], and P. CHERUBINI[1,3]

[1] *School of Natural Resources, University of Nebraska-Lincoln, USA*
[2] *The Nebraska Nature Conservancy, NE, USA*
[3] *Swiss Federal Institute for Forest, Snow and Landscapes, Switzerland*
* Corresponding Author: Tawada2@unl.edu

Keywords: paper birch, tree rings, riparian, MODIS, Landsat, NDVI, water, temperature, Nebraska Sandhills

Accepted for publication in Canadian Journal of Forest Research,
https://doi.org/10.1139/cjfr-2018-0206
Submitted May 16, 2018.
Published on the web 13 December 2018.

Abstract

Remnant populations of *Betula papyrifera* have persisted in the Great Plains after the Wisconsin Glaciation along the Niobrara River Valley, Nebraska. Population health has declined in recent years, and has been hypothesized to be due to climate change. We used dendrochronological techniques to assess the response of *B. papyrifera* to microclimate (1950-2014), and satellite imagery [Landsat 5 TM (1985-2011) and MODIS (2000-2014)] derived NDVI as a proxy for population health. Growing-season streamflow and precipitation were positively correlated with raw and standardized tree-ring widths and basal area increment increase. Increasing winter and spring temperatures were unfavorable for tree growth while increasing summer temperatures were favorable in the absence of drought. The strongest predictor for standardized tree-rings was the Palmer Drought Severity Index, suggesting that *B. papyrifera* is highly responsive to a combination of temperature and water availability. The NDVI from vegetation community was positively correlated with standardized tree-ring growth, indicating the potential of these techniques to be used as a proxy for ex-situ monitoring of *B. papyrifera*. These results aid in forecasting the dynamics of the species in the face of climate variability and

change in both remnant populations and across its current distribution in northern latitudes of North America.

1. Introduction

Paper birch (*Betula papyrifera* Marshall) is a widely distributed deciduous tree species across continental North America. It grows in the boreal forest from Newfoundland in eastern Canada all the way to northwestern Alaska in the U.S., crossing the Canadian prairies in Manitoba, Saskatchewan and Alberta. *B. papyrifera* also extends south from Washington in the western U.S. to Montana, and through the Great Lake States to New England in the eastern U.S. Scattered populations can be found in the Great Plains of Montana and North Dakota, the Black Hills of South Dakota, the Appalachian Mountains, and the Front Range of Colorado (Burns and Honkala 1990; map: http://nativeplantspnw.com/paper-birch-betula-papyrifera/). As a boreal species, *B. papyrifera* is adapted to the cold northern climate (USDA 1965; Stroh and Miller 2009), and has been found to have mixed responses to temperature especially during the growing season. Warming temperatures in the spring can result in an earlier bud burst

which can have positive impacts on growth due to increased cambial activity when water is available (Karlsson et al. 2004; Hollesen 2015; Li et al. 2016), but this comes with a risk of early season frost, which can damage and kill newly emerging buds and rootlets and may result in crown dieback (Pomerleau 1991). Water availability has also been shown to positively affect the performance of the species (Kharuk et al. 2014; Li et al. 2016). Water stress - including both excess water and drought - can cause defoliation (Wang et al. 2016), leading to suppressed tree-ring growth and performance for up to four years following defoliation (Karlsson et al. 2004).

After the Wisconsin Glaciation, remnant stands of *B. papyrifera* have persisted in the Great Plains but with declining presence (Wright 1970; Stroh and Miller 2009). One of these ecotypes is located along the Niobrara River Valley in north-central Nebraska, where the species can be found in north-facing canyons and along river banks. The valley plays an important ecological role as an ecotone where grassland and forest species converge, supporting a diverse array of vegetation that is rarely found in close proximity elsewhere (Stroh and Miller 2009). Short grass species from the semi-arid grasslands of the surrounding Sandhills, as well as grasses representing the mixed and tall grass

prairies can be found alongside forest species representing the western coniferous, eastern deciduous and boreal communities.

On a continental scale, one of the main threats to *B. papyrifera* has been increased climate variability, specifically temperature and precipitation. The species rarely occurs in areas where average July temperature exceeds 21˚C (Stroh and Miller 2009). In comparison, the Niobrara River Valley July average temperature is approximately 23.8˚C. Stroh and Miller (2009) attributed the health of the Niobrara River Valley populations to a cooler localized microclimate and the close proximity to the river bank. They reported dieback of *B. papyrifera* in recent years which is thought to have started around the 1980s, and possibly attributed to temperature increase.

Dendrochronological techniques can be applied to investigate ecological processes and tree responses to site conditions, which are then related to tree performance and forest productivity and health (Cherubini et al. 2002). Factors, such as site characteristics, abiotic and biotic environment, management practices, species growth habits, and genetics have been reported to influence the formation and growth of tree rings, and thus forest productivity (e.g., Schweingruber 1996; Di Matteo et al. 2010; Aus der Au et al. 2018). The normalized difference

vegetation index (NDVI) is another tool that is commonly used in remote sensing applications as a measure of photosynthetic activity, which can then be related to plant health and growth, through examining the ratio of spectral reflectance between the red and near-infrared regions of the electromagnetic spectrum (Vicente-Serrano et al. 2016). The few studies that have explored the relationship between NDVI and tree rings in the literature have shown that the relationship depends on vegetation type, spatial scale, period of study, and the abiotic and biotic environments (Bunn et al. 2013; Vicente-Serrano et al. 2016; Bhuyan et al. 2017). While tree rings studies are important for quantifying long-term variability in forest productivity, preparing the chronologies can be time consuming, and costly on a large scale. On the other hand, NDVI provides a good measure for landscape photosynthetic activity and site productivity and can be used to monitor landscape processes on a regular basis. Therefore, investigating how these two techniques relate to each other can improve our understanding of forest growth and productivity, carbon budgets and forests response to climate variability and change (Bhuyan et al. 2017).

At present, few studies have attempted to correlate tree rings with NDVI (Bhuyan et al. 2017), and even fewer have been conducted on this remnant *B. papyrifera* ecotype (Stroh and Miller 2009). It is unknown how climate fluctuations impact the performance of this species. The aims of this research are to: 1) use dendrochronological techniques to assess the past responses and performance of *B. papyrifera* to intra- and inter-annual microclimatic variability; and 2) determine if satellite imagery can serve as a proxy for assessing tree health by relating vegetation indices like NDVI to tree-ring characteristics. This study focuses on a time period spanning between 1950 and 2014. Results can have management implications and are important for the development of biogeographical and ecophysiological predictive models aimed at forecasting the dynamics and performance of this species in the face of future climate variability and change in both remnant populations and across its current habitat range in northern latitudes.

2. Materials and methods

2.1. Sites selection

The study area was located at the Nature Conservancy Niobrara Valley Preserve north-central Nebraska, centered at 42°78’34”N, 100°02’80”W and encompasses nearly 227 km^2 (Fig. 1). Seven north-facing *B. papyrifera* stands were selected along a 27 km section

of the river owned by The Nature Conservancy. The valley is 60 to 90 m deep, and ranges between 0.8 and 3.2 km in width. The water flow in the adjacent Niobrara River and its tributaries is in part determined by groundwater contribution (Szilagyi et al. 2002), as the groundwater flows over bedrock, therefore creating a high water table. Soil type is mostly alluvial fine-grained sand with a small amount of coarser material (Cady and Sherer 1946). Water moves in an easterly direction at a rate of roughly 0.3 md^{-1} through aquifers at a downward slope of anywhere from 2.5-13 m per every kilometer of easterly travel (Bradley 1956).

Sites were identified visually and accessed via the river by a canoe. *B. papyrifera* individuals were mostly present close to the river as part of a deciduous woody species community. Individuals were found only on north-facing slopes and growing from pre-existing root crowns. We did not observe any new seedlings or saplings in examined sites. The upland plant community was dominated with coniferous species including *Pinus ponderosa* and the native invasive *Juniperus virginiana* mixed with grasses. Sites were marked and Global Positioning System (GPS) locations were acquired for all trees (Fig. 1).

2.2. Microclimate

Precipitation and temperature data were acquired from the Ainsworth and Springview weather stations, located less than 35 km away, via the High Plains Regional Climate Center (HPRCC), University of Nebraska-Lincoln (HPRCC, https://climod.unl.edu/). Long-term (1901-2015) annual precipitation ranged between 241 and 938 mm and averaged 572 mm (Figs. 2 and 3). January average minimum and maximum temperatures were -12.3 °C and 0.4 °C, respectively, and July average minimum and maximum temperatures were 16.5 °C and 31.2 °C, respectively (Fig. 3). Monthly and annual Palmer Drought Severity Index (PDSI) data were acquired from NOAA (https://www7.ncdc.noaa.gov/CDO/CDODivisionalSelect.jsp#), calculated for the region of north-central Nebraska. PDSI is effective in determining long-term drought and takes into account potential evapotranspiration (Fig. 2). Monthly streamflow rate was obtained from the USGS National Water Information System (https://waterdata.usgs.gov/nwis/uv/?site_no=06461500&agency_cd=USGS&referred_module=sw), Sparks NE (Station code: 06461500; 42°54'14"N, 100°26'13"W). The stream gauge is located approximately 30 km from the study sites (Fig. 3). USGS uses

the information from the gauges for decision making on water management and as a warning system during extreme weather events.

2.3. Tree-ring parameters

We selected the largest trees based on healthiest visual appearance and largest diameter measured at breast height (DBH; Fig. 4). A total of 180 cores, i.e., four cores from each of 45 trees were sampled, at 1.3 m from the base, at 90° around the trunk; representing the north, south, east, and west sides (Maeglin 1979). The oldest ring record dated back to 1894, with the majority of consistent records across trees rings dating back to the early 1950s, thus the time frame selection for this study. Cores were placed on trays, glued to wooden dowels and sanded flat and smoothed with 150, 220, 440, and 600 grit sandpaper. Cores from southern and western facing sides of the trunk were sent to the tree-ring dendrochronological laboratory, at the Swiss Federal Institute for Forests, Snow and Landscapes (WSL), Switzerland (the reason for sending half of the samples to WSL was to measure both width and carbon and oxygen isotope ratios in annual tree rings, unfortunately we did not have enough wood material per annual ring to perform the

isotope analysis). Northern and southern facing cores remained at the Forest Ecophysiology Lab at the University of Nebraska (UNL) where they were scanned at 3200 dpi and individual ring widths were measured to the nearest hundredth of a millimeter (0.01 mm) and crossdated with the Windendro software platform. At WSL, the rings were measured under a microscope to the nearest 0.01 mm using a linear table, "LINTAB" (Rinn 2003). The data were recorded, presented and analysed in TSAPWin (Time Series Analysis and Presentation, Frank Rinn, Heidelberg, Germany; Stokes and Smiley 1968; Rinn 2003). After visually crossdating each tree core (north, south, east, and west), each sample plot was visually crossdated in TSAPWin. Missing rings were inserted manually with a value of 0 to complete the chronology. The visually crossdated data were imported into CONFECHA for statistical analysis to check crossdating accuracy (Grissino-Mayer 2001). Additionally, we determined the *Gleichläufigkeit* (Glk) which is a measure of the year-to-year agreement between the interval trends of two chronologies based upon the sign of agreement and usually expressed as a percentage of cases of agreement (Eckstein and Bauch 1969), as well as the cross dating index (CDI) which is a combination of the Glk with the *t*-value of the chronology (Rinn 2003). Basal area increment (BAI) increase was calculated from raw tree-ring measurements. Raw tree-ring widths were standardized using the "detrendeR" package

(Campelo 2012). Input values for the detrending procedure were set to spline length 20 and bandwidth 0.65, $P < 0.05$. Standardization removes biological factors of the individual samples due to age, disturbance, stand density, and size, leaving a value influenced primarily by climate (Cook and Holmes 1986).

2.4. Tree-ring statistical analysis

Statistical analysis was carried out in R using linear mixed modeling through the package "Lme4" (Bates et al. 2015). In all models considered, independent variables were represented by monthly cumulative precipitation, monthly average streamflow, monthly (mean, maximum and minimum) temperatures, and annual Palmer Drought Severity Index (PDSI) with year, stand, and sample (tree ID) as random effects. Monthly inclusion began in the growing season of the previous year through October of the current year. All models considered 1950 - 2014 for the time period and individual trees considered as separate response variables. Through early model creation, all parameters of spatial distinction (i.e., slope, aspect, distance/elevation to ridgeline and river edge) were removed as they did not show any statistical significance. They were thus not considered

in the creation of final models.

Stepwise backward selection is a process wherein a model is selected by removing one variable each step of the process based on t-statistics of their estimated coefficients (UCLA 2006). It is useful for selecting models from a moderate-sized pool of all potential inclusions. Concerns arise from this method as variables that are significant to the project at hand may be removed in early selection. When this method is employed, one must give consideration to the legitimacy of the selected product from a real-life perspective (Burnham and Anderson 2002).

All variables for consideration were included in a “global model” from which variables were systematically removed. At every step, all variables were individually tested for inclusion or removal using a Chi-square test based on their P-value, and a new model was created using the significant variables ($P < 0.05$). This process was repeated until the highest calculated P-value of variable removal was $P < 0.05$. At this point, model selection was completed and the final model considered determined.

2.5. Landsat and MODIS NDVI image analysis

Landsat 5 Thematic Mapper (TM) offers a spatial resolution (30 m) image with 16-day repeat cycle between image acquisitions and data dating back to the 1980s which serves as a valuable information source on landscape patterns and conditions over the study area. Landsat TM-derived Normalized Difference Vegetation Index (NDVI) data were used in this study as a proxy of plant health and productivity. Images were acquired from Google Earth Engine using the "LANDSAT/LT5_L1T_32DAY_NDVI" dataset with the Landsat cloud score algorithm applied to every available scene through the growing season, March through October, from 1985 - 2011. Pixels identified as "cloud" or "primarily water" were removed. The NDVI was calculated as the ratio of reflectance between the red (R 630 - 690 nm) and near-infrared (NIR 760 - 900 nm) regions of the electromagnetic spectrum as [NDVI = (NIR - R)/(NIR + R)].

NDVI values fall within the range of -1 to 1. The series of Landsat-based NDVI images available during the March to October time period for each year were temporally stacked for each image pixel. The maximum NDVI value was selected at the pixel level for each individual year to represent a measure of annual productivity. A total of 16 annual, maximum NDVI images were produced and compared to annual tree ring measurements for each corresponding year. Years were excluded if they did not have adequate cloud-free Landsat imagery to calculate maximum NDVI values that could be used in this study. As a results, annual representative images comprised of

data from June, July, and August of 1988, 1990 - 2001, and 2003 - 2007 were used to create a raster of pixel-based correlation (Pearson's R^2) values against tree-ring widths.

While Landsat images provide a high spatial resolution, the drawback to using it comes by way of cloud obstruction. We applied similar methods for comparison to MODIS imagery which offers a consistent, high temporal resolution multispectral dataset useful for examining surface changes throughout the year with imagery recorded every 1 - 2 days since December 1999 to present at 250 - 1000 m pixel resolution. NDVI image data were acquired through Google Earth Engine from the MODIS Terra Daily NDVI (Image collection: 'MODIS/MOD09GA_NDVI') data set for all available dates between March and October from 2000 - 2014. Cumulative growing season NDVI from MODIS imagery (Reed et al. 1996; Li et al. 2015; Kumar and Mutanga 2017) has been shown to provide a stronger estimate of aboveground biomass, and seasonal productivity, than single-date NDVI. Summed NDVI through distinct portions of the growing season were also examined and correlated to tree-ring growth. NDVI images were "stacked" for the time periods of March - October (full growing season), March - May (early season), June - August (mid-season), August – October (late season), May, June, July, and August. "Summed-NDVI"

or "accumulated NDVI values" for each date for these growing season windows within a specific year, which is considered a spectral-based proxy of general vegetation productivity were correlated using the Pearson's R^2 at the pixel level with tree-ring width.

2.6. Relationships between tree rings and NDVI

Tree-ring chronologies have been shown to reflect a strong, significant correlation with NDVI in other studies (Jicheng and Xuemei 2005; Forbes et al. 2010; Bhuyan et al. 2017). Tree coverage in each stand was smaller than an individual pixel's area in either the Landsat (30 m) or MODIS (250 m) imagery, which resulted in much of the area being comprised of non-*B. papyrifera* land cover types. Landscape position of *B. papyrifera* in remnant populations on steep banks close to the river was an additional reason the remote sensing image pixels containing the tree stands could not be directly compared. The stands were located near water and many of the image pixels containing the tree stands were predominately covered by either water or shade from the steep river bank. In both cases, the spectral signal and resultant NDVI would be primarily representative of the water and shaded area rather than the actual conditions of the *B. papyrifera*. As a result, direct, pixel-level comparison between the NDVI image pixels and the ground data could not be compared. This required alternative areas of a different land cover type to be used as a productivity proxy to compare with the traditional tree-ring data.

To address this, we investigated whether we can establish a relationship of *B. papyrifera* and pixel-based NDVI signal during the peak growing season with a plot-based vegetation

in the adjacent community. If successful, this method can be then applied elsewhere to similar areas. The adjacent grasslands were partitioned into 8 plots (as shown in Fig. 7), across a series of management areas along the Niobrara Valley preserve for long-term monitoring. These plots included: rotational grazing (plots 1, 2, 3), patch-burn cattle grazing (plot 4), patch-burn cattle grazing, burned in 2015 (plot 5), unburned cattle grazing, control (plot 6), bison grazing, burned in 2015 (plot 7), and bison grazing, unburned (plot 8). In the patch-burn grazed areas, there were no fires in 2016, so the two grids in each site were in unburned (for at least several years) versus burned areas in 2015. The patch-burn cattle control site is unburned, but grazed season-long at the same stocking rate as the patch-burn cattle pasture. In the rotational grazing treatments, each pasture is grazed at a different time each year.

Each plot consisted of an 8 m x 6 m grid (8 east-west, 6 north- south) of GPS points encompassed in an area of 640 x 480 m^2. At each GPS point, a 1 m^2 quadrat was dropped and vegetation sampled. Canopy height, and percent cover of each vegetation functional group (grass, shrubs and forbs), as well as litter, standing dead and bare soil, were recorded. Topography and vegetation composition were considered in reference to pixel-

based NDVI and tree ring growth correlation of *B. papyrifera* to identify potential areas of proxy monitoring based on their vegetation and/or topographical characteristics. We calculated the Pearson's R^2 value between averaged annual ring growth (raw, standardized, BAI,) and the annual representative NDVI values at each pixel location over the observed area. The R^2 values were organized in a single raster representing the pixel-level correlation to growth.

3. Results

3.1. Site microclimate

Annual cumulative precipitation for the area during the study period of 1950 – 2014 averaged 573±18 mm. During the 65-year study period, annual precipitation did not show any increasing or decreasing trend over time, instead precipitation varied annually around the mean (Fig. 2). The majority (80-90%) of the annual precipitation fell during the growing season between April and September (Fig. 3). Average annual streamflow ranged between 17 and 26.5 m^3s^{-1} with a mean annual streamflow of 21.7±0.3 m^3s^{-1} (Fig. 3). During the study period, average annual streamflow declined over time, which was

significant at $P < 0.1$. Streamflow increased in the spring with snow melt, and declined in July through September with decrease in precipitation and increase in temperature and evapotranspiration demands, before increasing again in October (Fig. 3). Annual Palmer Drought Severity Index (PDSI) ranged from -4.9 to 6.7, with a long-term average of 0.9±0.3. During the study period, annual PDSI exhibited upward (wetting) trend, which was significant at $P < 0.1$ ($P = 0.054$) (Fig. 3). Despite this wetting trend, years of moderate to severe droughts were common and constituted around 32% of the 65-year period of study.

Average annual air temperature was 8.9±0.1 °C (Fig. 2), with January mean temperature ranging between -15.1 to 3.0 ºC, and showing a slight and statistically significant warming over time ($P < 0.01$). March maximum temperatures ranged between 1.8 and 17.6ºC and displayed a significant decreasing trend ($P = 0.048$; Fig. S1). July maximum temperatures ranged between 24.4 and 37.4 ºC, and did not show an increasing or decreasing trend. July mean temperature met or exceeded 21 ºC nearly every year except for 1992 (Fig. S1).

3.2. Tree-ring chronologies

Tree diameter was positively and significantly correlated with age (Fig. 4). Raw tree-ring widths averaged 1.21±0.02 mm yr^{-1}, and basal area increment increase (BAI) averaged 325.3±4.27 mm^2 yr^{-1} (Fig. 5). Both raw tree-ring widths and BAI exhibited a significant decline in growth over time ($P < 0.001$). This decrease can be attributed to the normal growth behavior of *B. papyrifera* in general, as growth is rapid for the first 30 years or so and then sharply declines through maturity (Burns and Honkala 1990). Additionally, as a tree ages, cambial tissue must be distributed over a greater surface area, which results in narrower rings, i.e., the geometrical age effect (Sillett et al. 2015). Data standardization resulted in the removal of any significant trends ($P = 0.74$), and indicated variability around the mean (0.99±0.006 mm) which reflected inter- and intra-annual fluctuations in the abiotic environment (Fig. 5). A decline in tree-ring growth rate was observed in six periods, early 1960s, mid 1970s, late 1980s, early 1990s, early 2000s, and in 2012. These reductions in growth were associated with near zero or negative (drought) annual PDSI, or in years with lower than average air temperatures. Above average tree-ring widths,

standardized ring widths, and BAI were observed during wet years or positive PDSI (e.g., 1983, 1995, and 2009).

3.3. Climate correlations

Previous and current year summer and fall streamflow were positively correlated with raw tree-ring widths, BAI, and standardized ring widths (Fig. 6). Generally, streamflow of previous July through fall of current year was significantly correlated with standardized tree-ring widths. High precipitation and streamflow rates during April of current and previous year seemed to have a negative effect on tree-ring growth. Increased air temperatures of both current and previous year were generally negatively correlated with all measured tree parameters, with few exceptions (Fig. 6). The strongest predictor for standardized tree ring width was PDSI, where values were significantly and positively correlated at $P < 0.05$ for both previous and current year. Linear mixed modeling (LMM) highlighted the importance of mid-season water availability of both previous and current year, early season temperature of the current year, and late-season temperature of both the previous and current year for tree-rings growth.

3.4. Comparison of climate correlation and LMM

The standardized ring-width model was the most relevant for our study. This model indicated only a negative influence of previous November precipitation on growth while the R^2 showed significant positive correlation with previous October and December precipitation (Table S2). Pearson's R^2 correlations were significantly ($P < 0.05$) negative for previous January and positive for current June, October, and November. Standardized tree-ring widths indicated a disagreement where the model showed late previous season precipitation as negatively impacting growth while the Pearson R^2 showed significant positive correlation to late season precipitation of both previous and current year. The LMM and climate correlations all considered virtually the same pool of variables yet produced slightly different results, while the overall results were similar. When using backwards selection, one must reconsider that variables can be dropped early in the model creation process which could later show significance. One must also consider the overall model as a whole and interpret its meaning within the ecological context of the data itself.

Temperature results from the LMM and Pearson R^2 were in general agreement. Increasing temperature in previous April and June showed significant negative correlation to standardized ring growth. The findings portrayed from the LMMs and Pearson R^2 correlations were that increasing winter and spring temperatures are unfavorable for growth while increasing summer temperatures are favorable in the absence of drought.

3.5. NDVI as a proxy for vegetation and *B. papyrifera* health

Vegetation composition adjacent to *B. paryrifera* stands were sampled for both groundtruthing, and to identify the vegetation, topography and management practices that would provide the highest correlation with tree rings (Fig. 7). Sampled plots were dominated by grasses (31.9 to 49% cover) and averaged 37.6 ± 0.9%. Forbs percent cover ranged between 5.4 and 20.7%, and averaged 11.5 ± 0.5%. Shrub percent cover ranged between 6.2 and 27.4% and averaged 17.8 ± 1.1%. Litter percent cover ranged between 36.7 and 67.2% and averaged 52.4±1.5%. Litter composition was significantly lower in plot 4 (38.4%) and plot 7 (36.1%) relative to the others. Standing dead vegetation percent cover ranged averaged 6.2±0.5%. Bare ground percent cover ranged between

28.8 and 54.5% and averaged 41.8±1.5%. Bare ground cover was significantly high in plots 4 (54%), 5 (54%), and 7 (53%) relative to others. Canopy height ranged between 26.9 and 41.6 cm and averaged 34.0±1.4 cm (Fig. 7).

Max-value Landsat 5 NDVI from all vegetation plots followed the standardized tree-rings growth trend of *B. papyrifera* (Fig. 8; Fig. S4). Average Pearson's R^2 correlation values ranged between 0.36 and 0.76. Plot-level correlation was highest in plot 2 for standardized ring width at 0.76, and lowest in plot 8 with 0.36. Regressing standardized ring widths as a function of maximum NDVI derived from Landsat 5, showed the highest correlation with R^2 of 0.81 (Fig. 9). A notable significant drop in Landsat max-value NDVI was observed in 2002. Climate records indicate this year as one of low precipitation, low streamflow, warm temperature, and drought, along with decreased ring growth from the collected *B. papyrifera* dendrochronological record. MODIS sum-NDVI for the periods of July, August, and August - October reflect the same notable drop in 2002 NDVI for all 8 plot locations as seen in the Landsat 5 max-value NDVI (data not shown).

The correlation rasters were made semi-transparent and overlain on a triangulated irregular networks (TIN, representative of the topographical characteristics of the land)

representation of topography, which allowed us to observe any relationship between topography and/or vegetation composition as characteristics for identifying other sites of comparative use. Based on R^2 values and vegetation communities within the 8 sampled plots on the Nature Conservancy property, there was no obvious link between vegetation type and NDVI correlation to ring growth, as plots that contained significant differences of population composition typically showed a lower mean R^2 value (e.g., Fig. S4). However, topography, similar to that of *B. papyrifera,* seemed to play a significant role in identifying the proxy; plots 2, 6, 5, and 3 are all located on rougher areas of the landscape with a greater variations in topographical relief and comprised the top half of mean R^2 values of standardized ring width to pixel-level max-value Landsat NDVI. Plots 4, 7, 1, and 8 were located on flatter ground and comprised the bottom half of R^2 values of standardized ring width to pixel-level max-value Landsat NDVI (Figs. S3 and S4). This observed topographical influence appeared to be unrelated to aspect or direction, rather better characterized by the land contour of the general area in question. MODIS sum-value NDVI showed the strongest relationships during July to both raw and standardized growth, and June-August to standardized growth, and there was a consistency of the

higher mean-correlated vegetation sampling plots and rough topography, which mostly agrees with the Landsat 5 TM max-value NDVI results at the plot level (correlations are not shown, Fig. S3).

Pixel-level correlation of raw tree ring-width and standardized tree-ring width between Landsat max-value NDVI and MODIS summed-value NDVI during the summer months showed very similar results when compared to topography and plot-level vegetation composition (Figs. S2 and S3).

4. Discussion

Annual average precipitation, temperature and summer (July) temperature have remained reasonably stable with no upward or downward trends over the study period. However, the area did experience a warming trend in January temperature over time (Fig. 2). In northern latitudes, warming winter and spring trends can lead to increased ring growth and treeline advancement into neighboring tundra areas (Kharuk et al. 2014), as well as wider seasonal rings created as a result of earlier bud burst and increased cambial growth associated with longer growing season (Karlsson et al. 2004; Hollesen et al. 2015;

Yang et al. 2017). In this study, we show that warming January air temperatures had a negative effect on growth. This may be due to the higher January minimum temperatures in Nebraska relative to more northern latitudes causing the species to cross a threshold, and/or to re-freezing of the roots which can ultimately lead to reduction in growth, tree damage (Greenidge 1953; Redmond 1955), or in some cases death (Pomerleau 1991). Water availability has also been shown to have a mixed effects on growth, its availability encourages establishment and growth of birch species (Li et al. 2016), while water excess (i.e., logging of soil) or drought have been shown to decrease leaf area of birch species (Wang et al. 2016). Such may be the case here as the standardized model highlights a negative growth effect from increased precipitation during previous November and current May, or late-previous and early-current season. The defoliation response to excess water may very well translate into problematic bud formation in previous season and bud-burst in the following spring. Standardized tree-ring widths followed PDSI very closely, which suggests that inter and intra-annual growth of *B. papyrifera* is strongly dependent on a combination of temperature and water availability, in that warm and wet conditions during the growing season facilitate more growth (Li et al. 2016). This can also be seen notably

by the rapid reductions in standardized ring width during years of low (dry) PDSI in the late 1980s to early 1990s and the early 2000's versus an increase in standardized growth during years of high (wet) PDSI in the early 1980s, mid 1990s, and late 2000s, which agrees with other studies (Karlsson et al. 2004; Li et al. 2016). Drought extremes are expected to increase in frequency and duration for the future of the Great Plains (Bathke et al. 2014), which may impact the health and performance of this remnant forest.

Climate correlations showed streamflow from April through November of both previous and current year to be significantly and positively related to growth, agreeing with inclusion of August streamflow of both current and previous year, but disagreeing with the negative influence of July streamflow to raw growth and BAI as displayed by the selected models (Table S2). This influence of streamflow on growth might be explained by some of the unique geology of the Niobrara River Valley in that the river water, which flows directly over bedrock, is fed by lateral (easterly) movement of groundwater (Szilagyi et al. 2002). We observed *B. papyrifera* only growing in close proximity to the water's edge in small pockets (Table S1). Combining the shallow fibrous root system of paper birch, and the influence of drought-related conditions on growth, close proximity of this species to

the water table, and access to precipitation water or streamflow are necessary for its success.

NDVI derived from satellite imagery via both Landsat 5 TM and MODIS satellites showed potential use as a proxy for ex-situ *B. papyrifera* growth monitoring through high Pearson's R^2 values between ring growth and NDVI at the pixel level. Based on R^2 values and vegetation communities within the 8 sampled plots, there was no obvious link between vegetation type and NDVI correlation to tree-ring growth. However, vegetation on topography, similar to that of *B. papyrifera,* played a significant role in identifying the proxy. Other studies have linked satellite NDVI to climate variables such as temperature, precipitation, and drought conditions (Baird et al. 2012; Gensuo and Epstein 2003), and tree-ring width to NDVI with mixed success (Coops et al. 1999; Forbes et al. 2010; Vincente-Serrano et al. 2016). For example, Bhuyan et al. (2017) noted a positive relationship between NDVI and tree rings in many forests in the Northern Hemisphere, however the strength of this relationship depended on spatial scale, forest type (e.g., better correlation of NDVI with tree rings of conifers than deciduous species), species phenology, climatic zones, and method of combining NDVI for analysis. Liang et al.

(2005) reported strong relationship between grasslands NDVI and *Picea meyeri* in the semi-arid region of northern China. They argued that in semi-arid regions, such relationship can be expected as both vegetation types are limited by seasonal precipitation. Similarly in this study, where water is a limiting factor, we found that using NDVI of adjacent pasture lands with similar topographical characteristics to that of *B. papyrifera's* can provide a reliable representation of tree performance.

5. Conclusion

Dendrochronological techniques were used to identify microclimatic drivers of *B. papyrifera* growth of the Niobrara River Valley. We found that intra- and inter-annual average and pattern of precipitation, temperature, streamflow and PDSI to be important for growth. Climate correlations and LMM analyses produced similar results with some disagreements, but with both methods agreeing that the strongest predictor for standardized tree-rings was the Palmer Drought Severity Index, suggesting that *B. papyrifera* is highly responsive to a combination of temperature and water. Increasing winter and spring temperatures were unfavorable for tree growth while increasing summer

temperatures were favorable in the absence of drought. Drought is expected to increase in frequency and duration for the future of the Great Plains (Bathke et al. 2014). Warming conditions are also expected in the northern latitudes (Soja et al. 2007), and have been shown to impact riparian ecosystems leading to decreased biomass of riparian species and overall species richness and diversity. Riparian communities that depend on groundwater are predicted to be replaced with more water-competitive upland communities (Strom et al 2011). Combining the shallow fibrous root system of *B. papyrifera*, and the influence of drought-related conditions on growth, the future of Niobrara River Valley *B. papyrifera* will be dependent on climate and water availability at key points during the growing season. Factors such as water pumping for irrigation purposes on upland sites, and expansion of woody species especially the encroachment of *Juniperus virginiana* (Awada et al. 2013) will affect the horizontal movement of water over bedrock and impact water availability for *B. papyrifera*, and should therefore be monitored.

High NDVI values derived from satellites images of adjacent grasslands correlated with *B. papyrifera,* indicating that vegetation that shares the same topographic relief is governed by similar

environmental constraints in semi-arid areas (i.e., water), and can be used as a proxy to monitor a sparsely populated and/or remote species growth ex-situ. Results from this study can aid in forecasting the dynamics and thresholds of this species in the face of climate change in both the remnant populations and across its current distribution in northern latitudes of North America.

ACKNOWLEDGEMENT

This study was supported by the McIntire Stennis Forest Research Funds, USDA. The authors would like to thank the staff of the Dendrochronology Laboratory of the Swiss Federal Institute for Forests, Snow and Landscape for their assistance with the tree ring samples. We thank the High Plains Regional Climate Center (HPRCC, UNL) for the climate data, Les Howard for creating the location map, and the Nebraska Nature Conservancy and its staff for providing access to the Reserve and data on upland sites. We are also grateful for the two anonymous reviewers for their comments on the manuscript.

REFERENCES

Awada, T., El-Hage, R., Geha, M., Wedin, D.A., Huddle, J.A., Zhou, X., Msanne, J., Sudmeyer, R.A., Martin, D.L., and Brandle, J.R. 2013. Intra-annual variability and environmental controls over transpiration in a 58-year-old even-aged stand of invasive woody *Juniperus virginiana* L. in the Nebraska Sandhills, USA. Ecohydrol. **6**: 731-740.

Aus Der Au, R., Awada, T., Battipaglia, G., Hiller, J., Saurer, M., and Cherubini, P., 2018. Tree rings of *Pinus ponderosa* and *Juniperus virginiana* show different responses to stand density and water availability in the Nebraska grasslands. Am. Midl. Nat. **180**: 18-36.

Bathke, D.J., Oglesby, R.J., Rowe, C.M., and Wilhite, D.A. 2014. Understanding and Assessing Climate Change: Implications for Nebraska. University of Nebraska Press. P 72.

Baird, R.A., Verbyla, D., and Hollingsworth, T.N. 2012. Browning of the landscape of interior Alaska based on 1986-2009 Landsat sensor NDVI. Can. J. For. Res. **42**: 1371-1382.

Bates, D., Maechler, M., Bolker, B., and Walker, S. 2015. Fitting linear mixed-effects models using lme4. J. Stat. Soft. **67**: 1-48.

Bhuyan, U., Zang, Z., Vicente-Serrano, S.M., and Menzel, A. 2017. Exploring relationships among tree-ring growth, climate variability, and seasonal leaf activity on varying time scales and spatial resolutions. Remote Sens. **9**: 526 https://doi.org/10.3390/rs9060526.

Bradley, E. 1956. Geology and groundwater resources of the upper Niobrara River Basin, Nebraska and Wyoming. US Geological Survey Water-Supply Paper, 1368.

Bunn, A.G. 2013. Comparing forest measurements from tree rings and a space-based index of vegetation activity in Siberia. Environ. Res. Lett. **8**: 035034

Burnham, K.P., and Anderson, D.R. 2002. Model Selection and Multimodel Inference: A Practical Information-Theoretical Approach. 2nd ed. New York: Springer-Verlag.

Burns, R.M., and Honkala, B.H. 1990. Silvics of North America. US Department of Agriculture – Forest Service.

Cady, R.C., Scherer, O.J. 1946. Geology and ground-water resources of Box Butte County, Nebraska. U. S. Geological Survey Water-Supply Paper 969.

Campelo, F. 2012. DetrendeR: Start the detrendeR Graphical User Interface (GUI). R package version 1.0.4. https://CRAN.R-project.org/package=detrendeR

Cherubini, P., Fontana, G., Rigling, D., Dobbertin, M., Brang, P., and Innes, J.L. 2002. Tree-life history prior to death: two fungal root pathogens affect tree-ring growth differently. J. Ecol. **90**: 839-850.

Cook E.R. AND R. L. HOLMES. 1986. Users' manual for program ARSTAN. Laboratory of Tree-Ring Research, University of Arizona, Tucson.

Coops, N., Bi, H., Barnett, P., and Ryan, P. 1999. Estimating mean and current annual increments of stand volume in a regrowth eucalypt forest using historical Landsat multi spectral scanner imagery. J. Sust. For. **9**(3-4):149.

Di Matteo, G., De Angelis, P., Brugnoli, E., Cherubini, P., and Scarascia-Mugnozza G. 2010. Tree-ring $\Delta^{13}C$ reveals the impact of past forest management on water-use efficiency in a Mediterranean oak coppice in Tuscany (Italy). Ann. For. Sci. **67**: 510.

Eckstein, D., and Bauch, J. 1969. Beitrag zur Rationalisierung eines Dendrochronologischen

Verfahrens und zur Analyse seiner Aussagesicherheit. Forstwirtschaftliches Zentralblatt, 88. Verlag Paul Parey, Hamburg.

Forbes, B.C., Fauria, M.M., and Zetterberg, P. 2010. Russian Arctic warming and 'greening' are closely tracked by tundra shrub willows. Glob. Change Biol. **16**: 1542-1554.

Gensuo, J.J., and Epstein, H.E. 2003. Greening of Arctic Alaska 1981-2001. Geophys. Res. Lett., **30**: 20.

Greenidge, K.N.H. 1953. Further studies of birch dieback in Nova Scotia. Can. J. Bot. **31**: 548-559.

Grissino-Mayer, H.D. 2001. Evaluating crossdating accuracy: A manual and tutorial for the computer program COFECHA. Tree-Ring Res. **57**: 205-221.

Hollesen, J., Buchwal, A., Rachlewicz, G., Hansen, B.U., Hansen, M.O., Stecher, O., and Elberling, B. 2015. Winter warming as an important co-driver for *Betula Nana* growth in Western Greenland during the past century. Glob. Change Biol. **21**: 2410-2423.

Jicheng, H., and Xuemei, S. 2005. Relationships between tree-ring width index and NDVI of grassland in Delingha. Chinese Sci. Bull. **51**:1106-1114.

Karlsson, P.S., Tenow, O., Bylund, H., Hoogesteger, J., and Weih, M. 2004. Determinants of mountain birch growth in situ: effects of temperature and herbivory. Ecography. **27**: 659-667.

Kharuk, V.I., Kuzmichev, V.V., Sergey, T., and Im Ranson, K.J. 2014. Birch stands growth increase in western Siberia. Scan. J. For. Res. **29**: 421-426.

Kumar, L., and Mutanga, O. 2017. Remote sensing of above-ground biomass. Remote Sens. **9**: 935.

Li, B., Heijmans, M.M.P.D., Berendse, F., Blok, D., Maximov, T., and Sass-klaassen, U. 2016. The role of summer precipitation and summer temperature in establishment and growth of dwarf shrub *Betula Nana* in Northeast Siberian Tundra. Polar Biol. **39**: 1245-1255.

Li, L., Guo, Q., Tao, S., Kelly, M., and Xu, G. 2015. LiDAR with multi-temporal MODIS provide a means to upscape predictions of forest biomass. ISPRS J. Photogram. Remote Sens. **102**: 198-208.

Liang, E.Y., Shao, X.M., and He, J.C. 2005. Relationship between tree growth and NDVI of grassland in the semi-arid grassland of north China. Intern. J. Remote Sens. **26**: 2901-2908.

Maeglin, R.R. 1979. Increment cores: How to collect, handle, and use them. General tech report, FPL 25, United States Forest Service.

NASA. 2000. Measuring Vegetation: NDVI and EVI. https://earthobservatory.nasa.gov/Features/MeasuringVegetation/measuring_vegetation_2.php. Accessed on September 2017.

Pomerleau, R. 1991. Experiments on the causal mechanisms of dieback on deciduous forests in Québec. Québec Region Canadian Forest Service, Information Report LAU-X-96, 47

Redmond, D.R. 1955. Studies in forest pathology: XV. Rootlets, mycorrhiza, and soil temperature in relation to birch dieback. Can. J. Bot. **33**: 595–627.

Reed, B.C., Loveland, T.R., and Tieszen, L.L. 1996. An approach for using AVHRR data to monitor U.S. Great Plains Grasslands. Geocarto Int. **11**: 13-22.

Rinn, F. 2003. TSAP-Win: Time Series Analysis and Presentation for Dendrochronology and Related Applications. Version 0.55 User reference. Heidelberg, Germany (http://www.rimatech.com).

Schweingruber, F. H. 1996. Tree rings and environment dendroecology. Paul Haupt., Bern, Stuttgard, Wien.

Sillett, S.C., van Pelt, R., Carroll, A.L., Kramer, R.D., Ambrose, A.R., and Trask D.A. .2015. How do tree structure and old age affect growth potential of California redwoods? Ecol. Monogr. **85:** 81-212.

Soja, A.J., Tchebakova, N.M., French, N.H., Flannigan, M.D., Shugart, H.H., Stocks, B.J., Sukhinin, A.I., Parfenova, E.I., Chapin III, S.F., and Stackhouse Jr., P.W. 2007. Climate-induced boreal forest change: predictions versus current observations. Glob Planet. Change. **56**: 274–296.

Stokes, M.A., and Smiley, T.L. 1968. An Introduction to Tree-ring Dating. University of Arizona Press, Tucson, AZ.

Stroh, E.D., and Miller, J.P. 2009. Paper birch decline in the Niobrara River Valley, Nebraska: weather, microclimate, and birch stand conditions. U.S. Geological Survey Open-file Report 2009–1221.

Strom, L., Jansson, R., Nilsson, C., Johansson, M.E., and Xiong, S. 2011. Hydrologic effects on riparian vegetation in a boreal river: an experiment testing climate change predictions. Landscape Ecology Group, Department of Ecology and Environmental Science, Umed University.

Szilagyi, J., Harvey, F.E., and Ayers, J.F. .2002. Regional estimation of base recharge to ground water using water balance and a base-flow index. Ground Wat, **41**: 504-513.

UCLA. 2006. Introduction to Generalized Linear Mixed Models, UCLA: Statistical Consulting Group. http://stats.idre.ucla.edu/other/mult-pkg/introduction-to-generalized-linear-mixed-models. Accessed 15 September 2017.

U.S. Department of Agriculture (1965) Silvics of forest trees of the United States: Forest Service Agricultural Handbook No. 271.

Vincente-Serrano, S.M., Camarero, J.J., Olano, J.M, Martin-Hernandez, N., Pena-Gallardo, M., Tomas-burguera, M., Gazol, A., Azorin-Molina, C., Bhuyan, U., and El Kenawy, A. 2016. Diverse relationships between forest growth and the normalized difference vegetation index at a global scale. Rem. Sens. Environ. **187**: 14-29.

Wang, A.F., Roitto, M., Sutinen, S., Lehto, T., Heinonen, J., Zhang, G., and Repo, T. 2016. Waterlogging in late dormancy and the early growth phase affected root and leaf morphology in *Betula pendula* and *Betula pubescens* Seedlings. Tree Physiol. **36**: 86-98.

Wright, H.E. 1970. Vegetational history of the central plains. In: Dort, W., Jones, J.K. (eds) Pleistocene and Recent Environments of the Central Great Plains: Lawrence, University of Kansas Press, p. 157–172.

Yang, B., He, M., Shishov, V., Tychkov, I., Vaganov, E., Rossi, S., Ljungqvist, F.C., Brauning, A., and Grießinger, J. 2017. New perspective on spring vegetation phenology and global climate change based on Tibetan plateau tree-ring data. PNAS. **114**: 6966-6971.

Figures Caption:

Figure 1. Location of the study area along the Niobrara River Valley in north-central Nebraska, USA. Locations of the examined *Betula papyrifera* stands are marked with black dots.

Figure 2. Annual precipitation, average air temperature, streamflow, and Palmer Drought Severity Index (PDSI) for the study area along the Niobrara River Valley in north-central Nebraska. Dashed lines describe the parameter trend over time.

Figure 3. Long-term average monthly streamflow of the Niobrara River (m^3s^{-1}), air temperature (°C), and precipitation (mm) between 1950 and 2014.

Figure 4. Diameter at breast height (DBH) as a function of age of *B. papyrifera* trees.

Figure 5. Average annual (A) raw tree ring width (mm), (B) basal area increment increase (mm^2), and (C) standardized ring width (mm) of *B. papyrifera* along the Niobrara River Valley between 1950 and 2014.

Figure 6. Pearson R^2 correlation of tree ring width (Raw), basal area increment increase (BAI) and standardized tree ring growth (Std) of *B. papyrifera,* as a function of previous and current year precipitation, streamflow, temperature, and PDSI, along the Niobrara River Valley, NE between 1950 and 2014. * = significance at $P < 0.1$, and ** = significance at the $P < 0.05$.

Figure 7. Vegetation sampled from 8 plots located across a series of management treatments on the Niobrara Valley Preserve, The Nature Conservancy on June 27, 2016. Each plot consists of an 8 x 6 grid (8 east - west, 6 north - south) of GPS points encompassed in a 640m x 480m area. The bar-plot on the left shows percent cover of litter, standing dead vegetation, grass, forbs, and bare soil. Map on the right shows the location of the plots relative to sampled trees (white dots).

Figure 8. Average standardized growth of *B. papyifera* and max-value Landsat-5 NDVI between 1985 and 2011 within the 8 640m x 480m vegetation composition plots sampled in June, 2016 by the Nature Conservancy at the Niobrara Valley Preserve in Nebraska.

Figure 9. Standardized ring width of *B. papyrifera* as a function of maximum Landsat-5 NDVI observed in adjacent plots in Niobrara River Valley between 1985-2011. Missing points are due to cloud cover.

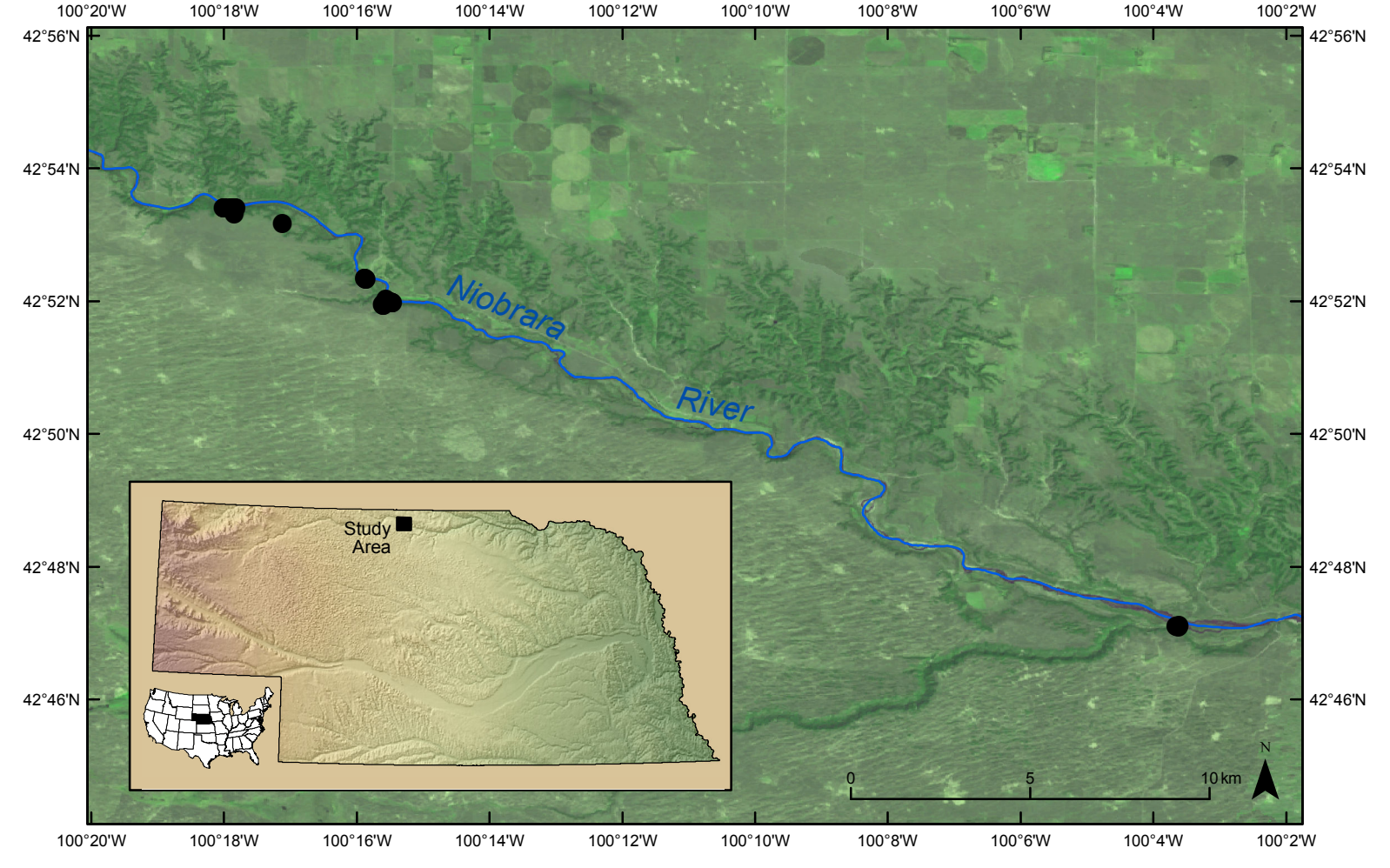
100°20'W
100°18'W
100°16'W
100°14'W
100°12'W
100°10'W
100°8'W
100°6'W
100°4'W
100°2'W
42°56'N
42°54'N
42°52'N
42°50'N
42°48'N
42°46'N
Niobrara
River
Study
Area
0
5
10 km
N

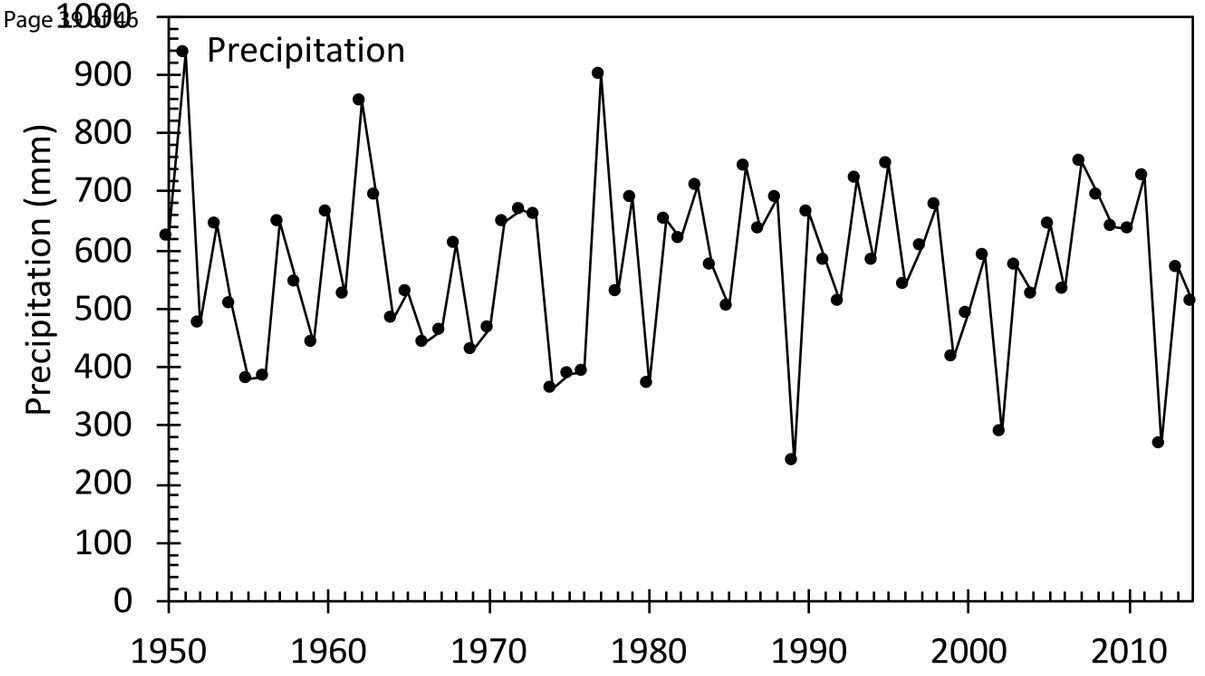
Precipitation
Precipitation (mm)
1000
900
800
700
600
500
400
300
200
100
0
1950
1960
1970
1980
1990
2000
2010

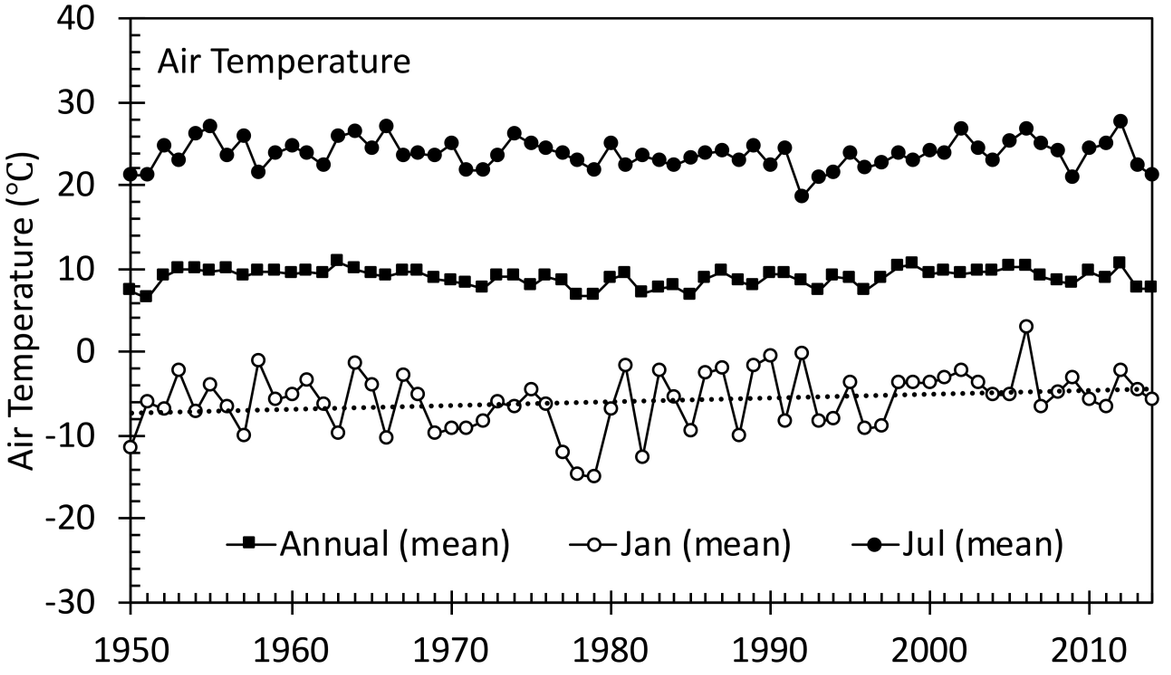
Air Temperature
Air Temperature (°C)
40
30
20
10
0
-10
-20
-30
Annual (mean)
Jan (mean)
Jul (mean)
1950
1960
1970
1980
1990
2000
2010

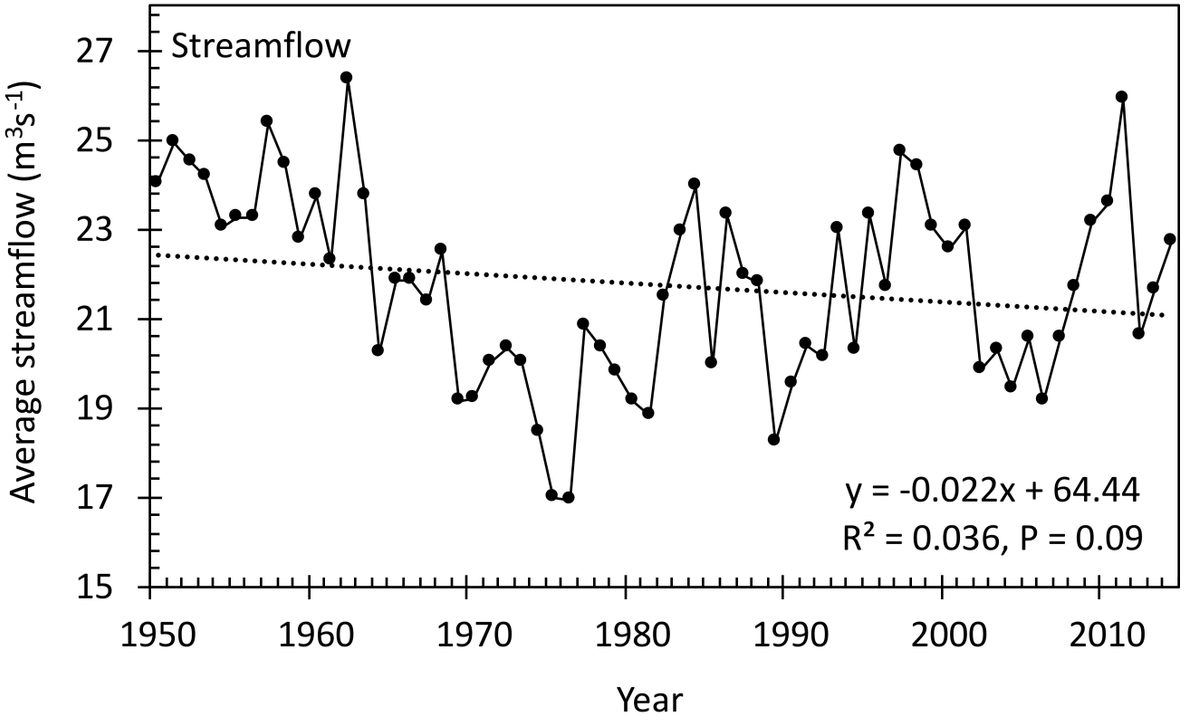
Streamflow
Average streamflow (m3s-1)
27
25
23
21
19
17
15
y = -0.022x + 64.44
R² = 0.036, P = 0.09
1950
1960
1970
1980
1990
2000
2010
Year

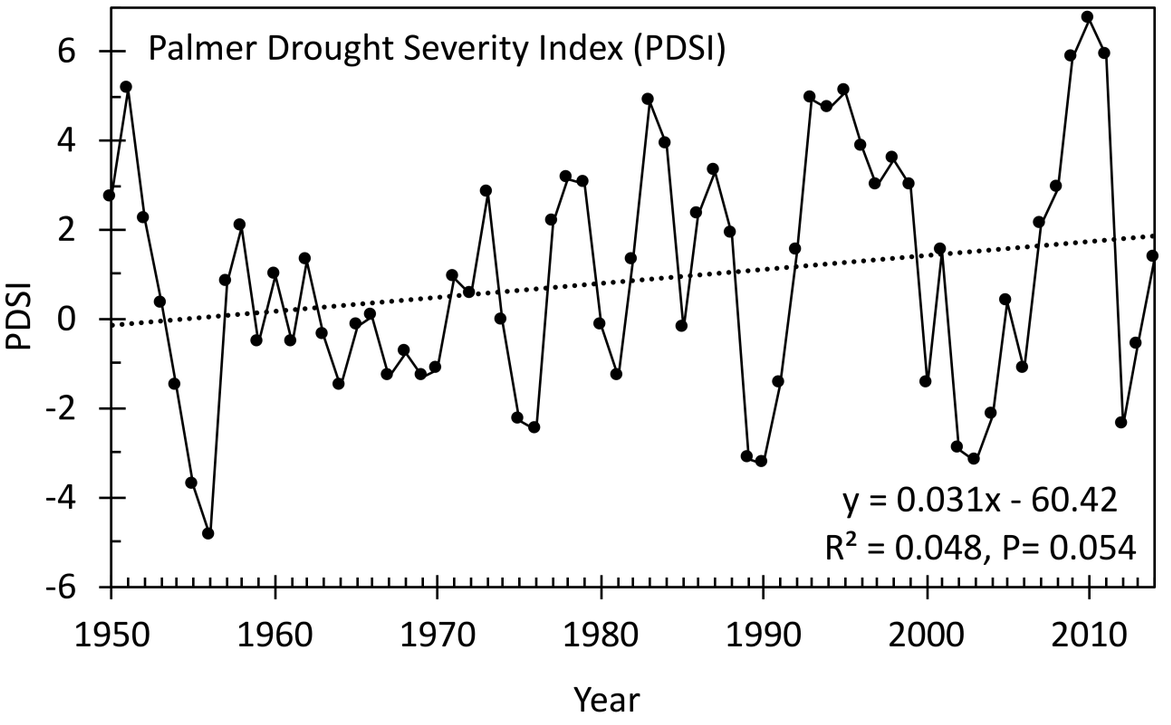
Palmer Drought Severity Index (PDSI)
PDSI
6
4
2
0
-2
-4
-6
y = 0.031x - 60.42
R² = 0.048, P= 0.054
1950
1960
1970
1980
1990
2000
2010
Year

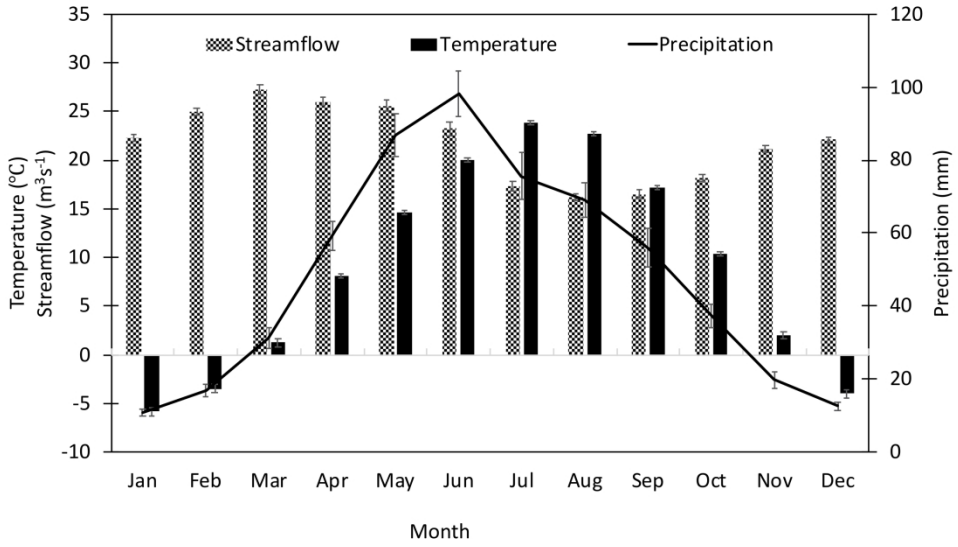

Figure 3. Long-term average monthly streamflow of the Niobrara River (m3s-1), air temperature (□C), and precipitation (mm) between 1950 and 2014.

255x142mm (300 x 300 DPI)

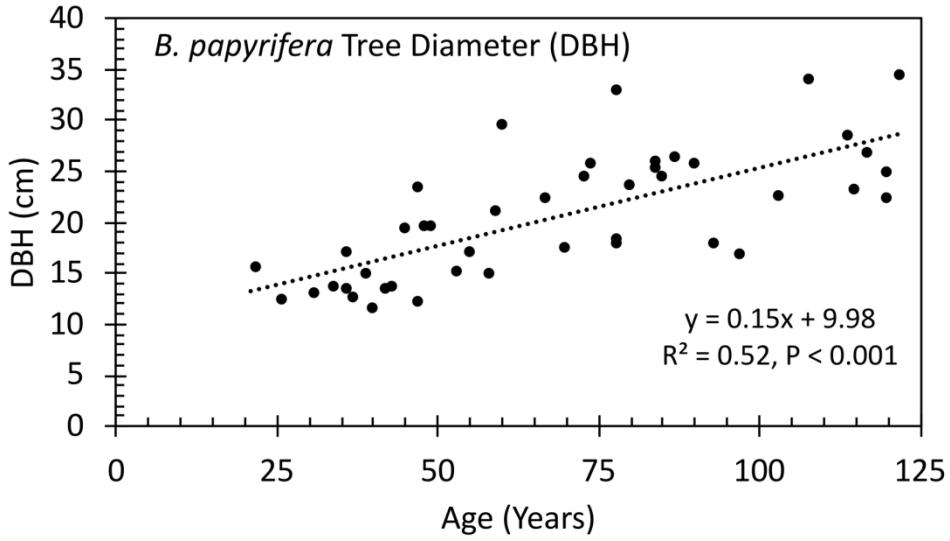

Figure 4. Diameter at breast height (DBH) as a function of age of B. papyrifera trees.

163x91mm (300 x 300 DPI)

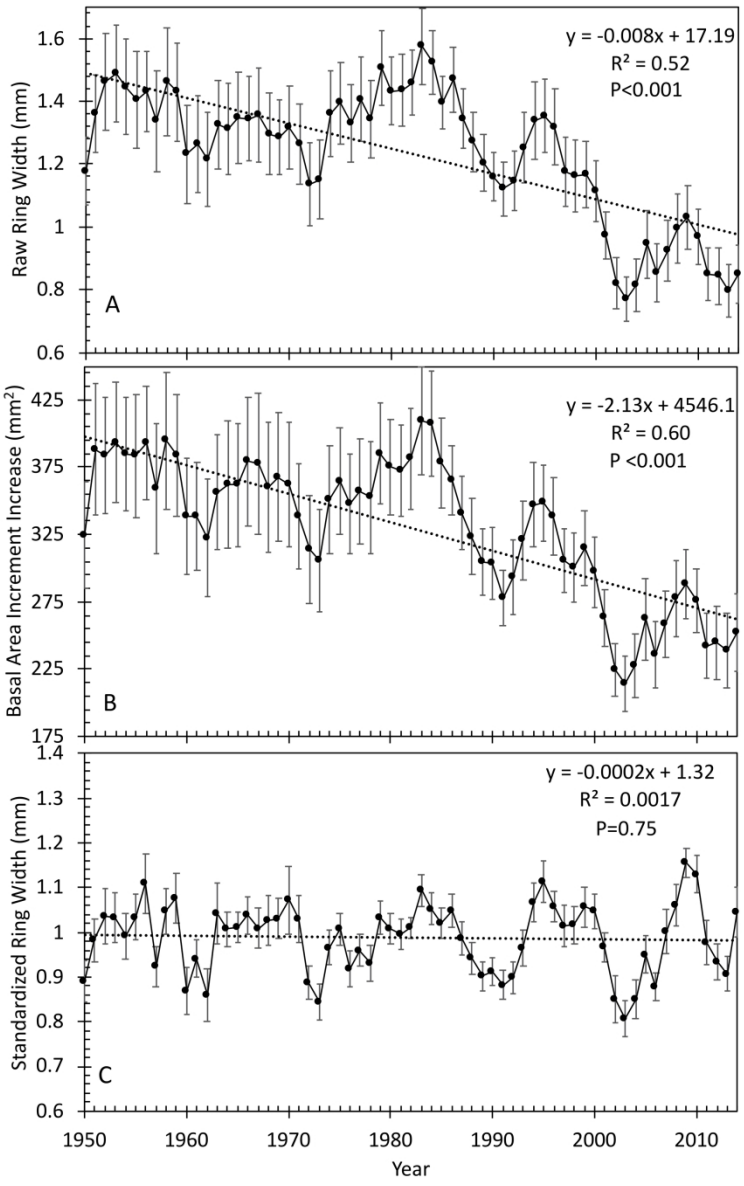

Figure 5. Average annual (A) raw tree ring width (mm), (B) basal area increment increase (mm2), and (C) standardized ring width (mm) of B. papyrifera along the Niobrara River Valley between 1950 and 2014.

201x306mm (300 x 300 DPI)

Current Year Precipiation
Pearson correlation
0.5
0.4
0.3
0.2
0.1
0
-0.1
-0.2
-0.3
-0.4
-0.5
Raw
BAI
Std
Jan Feb Mar Apr May Jun Jul Aug Sep Oct Nov Dec

Previous Year Precipitation
0.5
0.4
0.3
0.2
0.1
0
-0.1
-0.2
-0.3
-0.4
-0.5
Raw
BAI
Std
Jan Feb Mar Apr May Jun Jul Aug Sep Oct Nov Dec

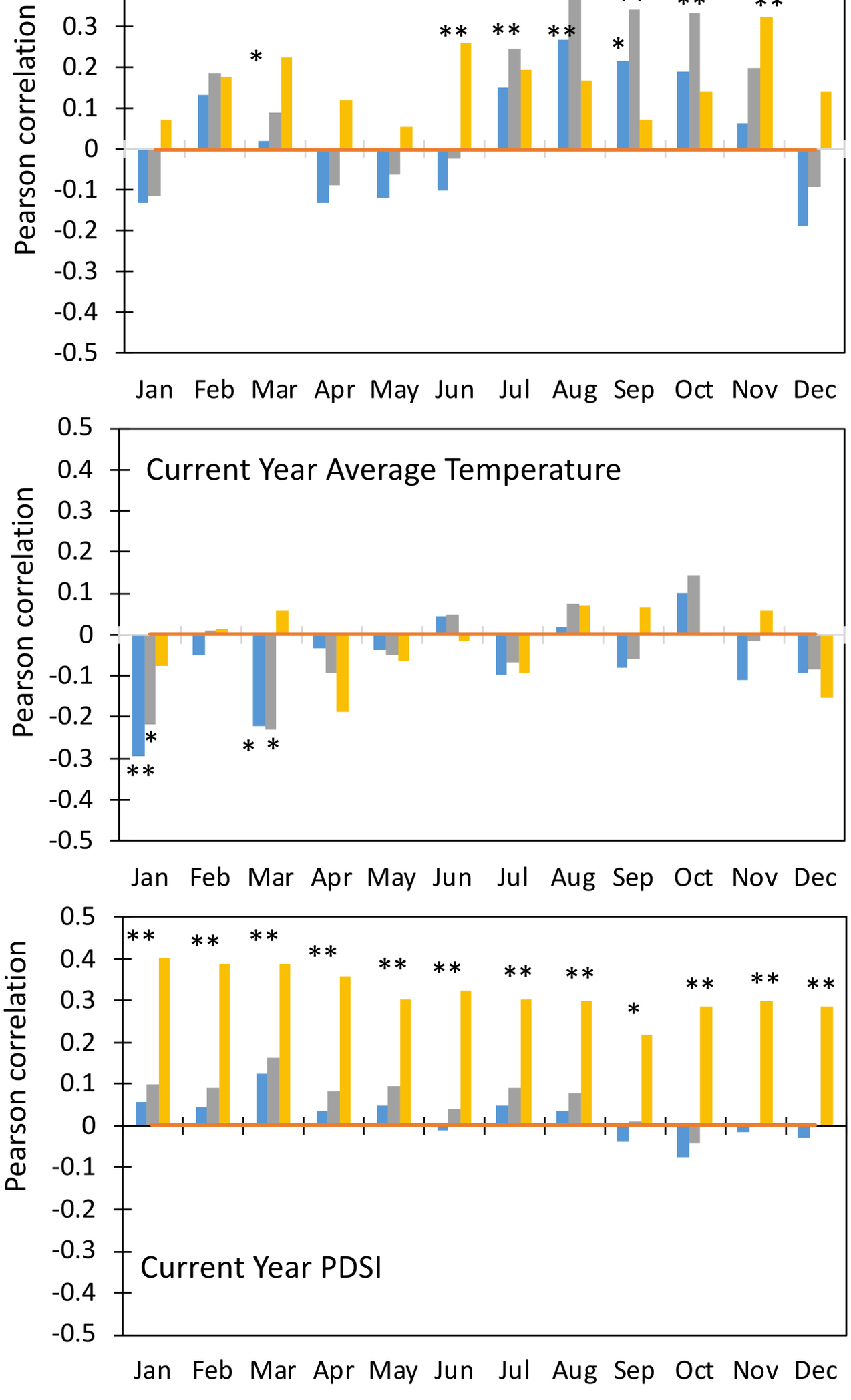
Current Year Streamflow
Pearson correlation
0.5
0.4
0.3
0.2
0.1
0
-0.1
-0.2
-0.3
-0.4
-0.5
Jan Feb Mar Apr May Jun Jul Aug Sep Oct Nov Dec

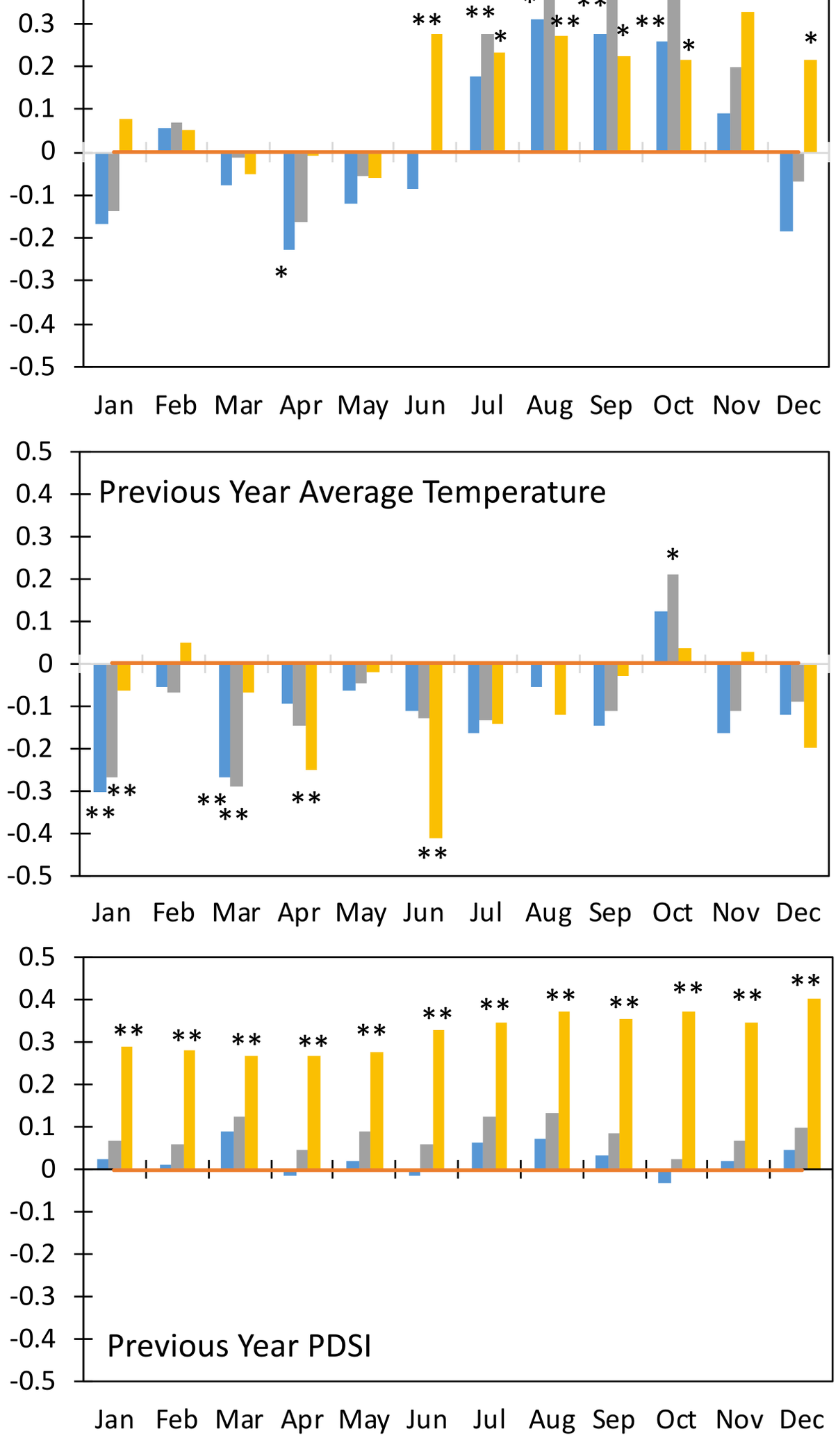
Previous Year Streamflow
0.5
0.4
0.3
0.2
0.1
0
-0.1
-0.2
-0.3
-0.4
-0.5
Jan Feb Mar Apr May Jun Jul Aug Sep Oct Nov Dec

Current Year Average Temperature
Pearson correlation
0.5
0.4
0.3
0.2
0.1
0
-0.1
-0.2
-0.3
-0.4
-0.5
Jan Feb Mar Apr May Jun Jul Aug Sep Oct Nov Dec

Previous Year Average Temperature
0.5
0.4
0.3
0.2
0.1
0
-0.1
-0.2
-0.3
-0.4
-0.5
Jan Feb Mar Apr May Jun Jul Aug Sep Oct Nov Dec

Current Year PDSI
Pearson correlation
0.5
0.4
0.3
0.2
0.1
0
-0.1
-0.2
-0.3
-0.4
-0.5
Jan Feb Mar Apr May Jun Jul Aug Sep Oct Nov Dec

Previous Year PDSI
0.5
0.4
0.3
0.2
0.1
0
-0.1
-0.2
-0.3
-0.4
-0.5
Jan Feb Mar Apr May Jun Jul Aug Sep Oct Nov Dec

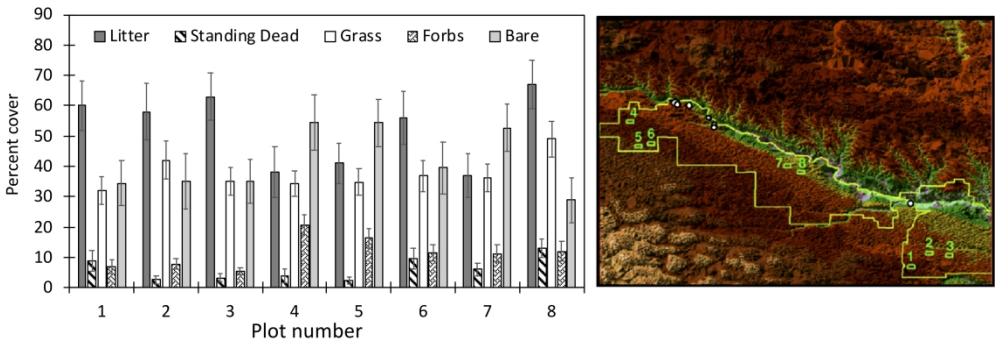

Figure 7. Vegetation sampled from 8 plots located across a series of management treatments on the Niobrara Valley Preserve, The Nature Conservancy on June 27, 2016. Each plot consists of an 8 x 6 grid (8 east - west, 6 north - south) of GPS points encompassed in a 640m x 480m area. The bar-plot on the left shows percent cover of litter, standing dead vegetation, grass, forbs, and bare soil. Map on the right shows the location of the plots relative to sampled trees (white dots).

306x112mm (300 x 300 DPI)

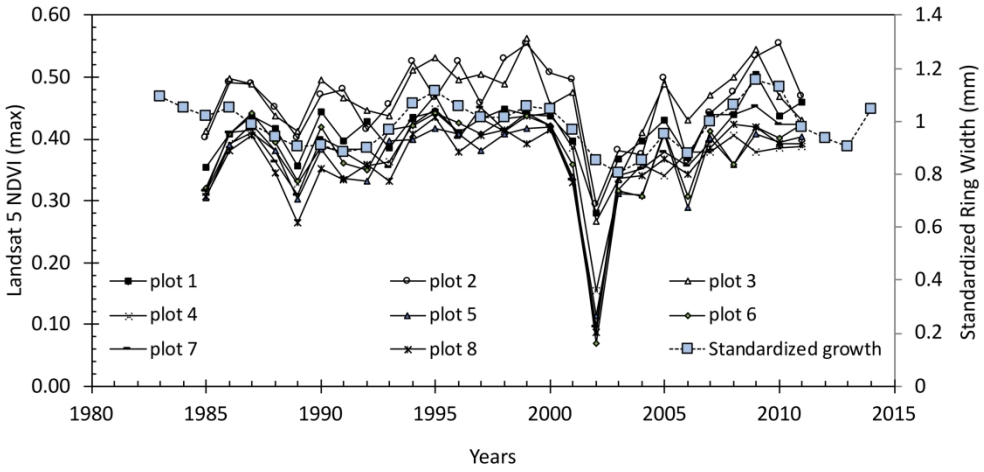

Figure 8. Average standardized growth of B. papyifera and max-value Landsat-5 NDVI between 1985 and 2011 within the 8 640m x 480m vegetation composition plots sampled in June, 2016 by the Nature Conservancy at the Niobrara Valley Preserve in Nebraska.

253x138mm (300 x 300 DPI)

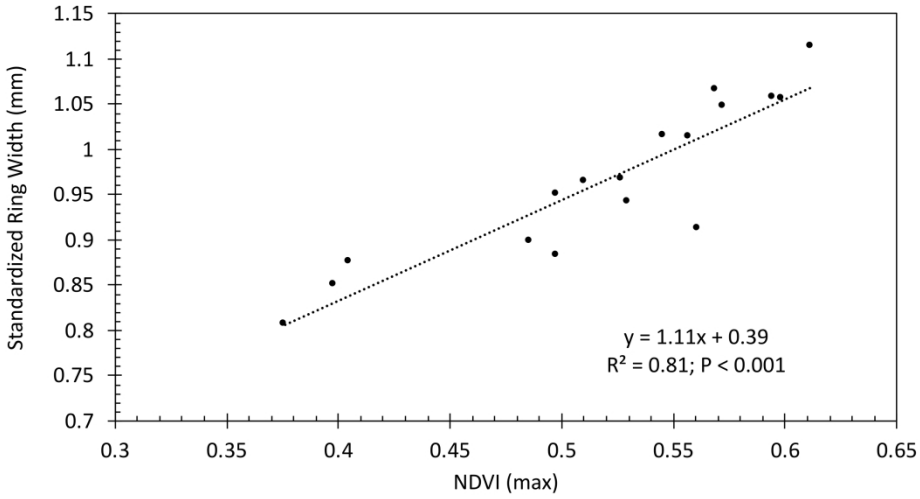

Figure 9. Standardized ring width of B. papyrifera as a function of maximum Landsat-5 NDVI observed in adjacent plots in Niobrara River Valley between 1985-2011. Missing points are due to cloud cover.

277x168mm (300 x 300 DPI)